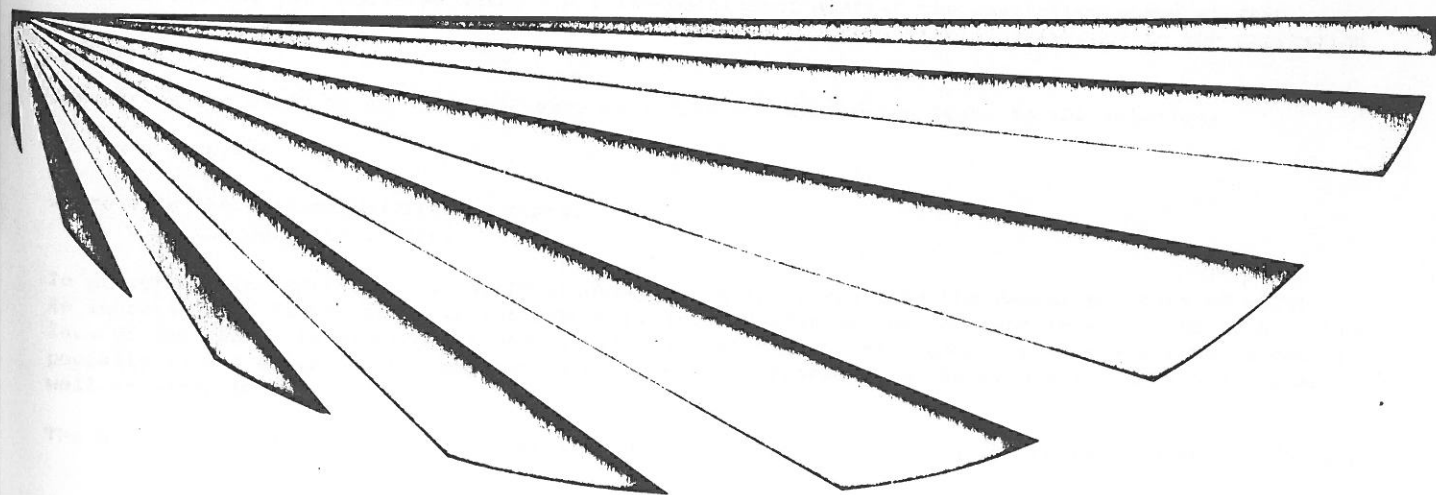


Conference Papers

High-Speed Surface Craft Exhibition & Conference

Incorporating the 3rd International Hovering Craft and Hydrofoil Exhibition



24-27 June 1980 Metropole, Brighton, Sussex, United Kingdom

HIGH-SPEED SURFACE CRAFT

A RECORD OF PROGRESS MADE ON A PURPOSE BUILT HYDROFOIL SUPPORTED SAILING TRIMARAN

N. Bose & R.C. McGregor

Department of Naval Architecture & Ocean Engineering, Glasgow University.

The paper describes the development of the foil system design from previous work (Bose 1978) in which an earlier vessel was tank and loch tested at full scale. The trimaran has four foils, bow and stern foils on the centre hull and one on each float. All except the stern foil are made up of dihedral elements. The stern foil is an inverted Tee set at zero incidence and is designed to provide some measure of trim control in addition to steering.

An iterative computer design program has been developed based on surface piercing hydrofoil theory and using this, estimates of drag, trim, flight displacement and lift/drag ratio have been made for various adjustments in the hydrofoil system design. Comparisons have also been made with other sailing hydrofoil craft.

The comparison between open water tests and the theoretical and tank results should provide a predictive method for generalised foil systems in sailing hydrofoils.

INTRODUCTION

The preliminary design of the hydrofoil boat described herein was based on development work on a previous hydrofoil boat which is described fully in references (1), (2). The trimaran 'Kaa' with her first generation foil system has already been launched and was tested at the Weymouth speed trials in October 1979 (3). The fastest timed run was recorded as 10.9 knots (5.6 m/s), but faster speeds were realised at times. Unfortunately 'Kaa' damaged her leeward foil during a foilborne trial while travelling around 15 knots (7.7 m/s) and subsequently completed the remaining third of the course to average 10.5 knots overall. This incident caused the boat to sink slowly and she was later rescued and towed in. Details of this boat with her 'Weymouth' foil configuration are given in Table I and Fig. 1.

THE FOIL SYSTEM DESIGN

The following requirements led to a starting point in the hydrofoil design spiral.

(1) Take-off speed

The take-off speed was chosen to be 6-7 knots.

(2) Maximum speed and foil sections

A maximum speed in the 30-40 knot range was also decided upon. This choice had a bearing on foil section selection since for the range of angles of incidence required at this speed, a comparison between different foil sections could be made by referring to cavitation 'bucket' diagrams (5). In Fig. 2 curves are shown for NACA sections 16-1012, 16-412 and Gö 14K, the two former being the sections chosen, the abscissae being 2-D lift coefficient against the cavitation speed at zero depth. The small depths at which these foils operate makes very little difference to the cavitation speed.

The curves are based on a vapour pressure of $1.72 \times 10^3 \text{ N/m}^2$ which leads to the relation:

$$v = 13.9/\sqrt{\sigma}$$

where σ is the critical cavitation number
 v is the velocity in m/s.

In practice this expression is fairly insensitive to the changes in the vapour pressure of water. An increase of a factor of 10 in the vapour pressure decreases the constant from 13.9 to 12.8. This lack of dependence is significant because wide variations in the vapour pressure are experienced especially in sea water due to temperature changes and variations in the amount of entrained air as well as other impurities.

The NACA 16-1012 section which will be free of cavitation up to 14 m/s (27 knots) was chosen for the

HIGH-SPEED SURFACE CRAFT

lower speed take-off foils whereas the NACA 16-412 was used for higher speed foils such as the cantiliver portions of the side foil units. In practice, the width of the 'buckets' is larger than that drawn as this marks the boundary at which the pressure just falls to vapour pressure. There is evidence that cavitation is delayed beyond this point (8) and this is also suggested by the experimental curve for GÖ 14K (9) which is a very similar section to NACA 16-412. In any case a limited amount of cavitation may be tolerated. The width of the 'bucket' is important in determining the operating range of angles of incidence. This range needs to be particularly high for sailing hydrofoils as they are not only subject to variations caused by wave motions, but to leeway angles also. Theoretically these considerations can lead to cavitation difficulties at much lower speeds than in motor hydrofoil craft, and possibly also aggravate the initiation of ventilation. Three dimensional and surface considerations reduce the likelihood of cavitation by pressure relief on the suction side of the foils. However, on the larger aspect ratio foil elements at mid-span, pressures may approach those experienced on 2-D foils and so the 2-D results are used as the criterion.

(3) Longitudinal and lateral stability

The requirements in this area stem from operation in waves (4,6), together with forces from the sail system necessitate the use of 'stiff' foils. For surface piercing foils this requires relatively high dihedral angles to be selected for the bow and side foil units.

(4) Trim control

An inverted tee foil, set at zero degrees incidence, was selected for the stern foil and acts as a trim control device.

(5) Crew

A regular crew of two was accepted as necessary for continuous control, but higher speeds over short distances were envisaged with only one crew member on board.

(6) The drag hump

In a sailing hydrofoil minimum drag at take-off is necessary, irrespective of the drag experienced at higher speeds. The boat may be able to sail faster in high wind speeds, but it must still be able to take-off at relatively low wind speeds. (This is in contrast to the powered hydrofoil concept where a fixed maximum power is available, accessible at all times, and the drag hump can be as high as the drag at the maximum speed so long as acceptable lift/drag ratios are achieved at the cruising speed.)

(7) C.L.R./C.E. criterion

The centre of lateral resistance (C.L.R.) must be suitably located relative to the centre of effort (C.E.) of the sails to provide adequate manoeuvrability under sail.

This last point, together with that of providing adequate reserve of lift at the bow foil unit, had a strong influence on the final choice of overall configuration, and the design was eventually based on a trimaran system of hulls, with one bow and stern foil mounted on the centre hull and a side foil mounted on each float around the midships position. Details of this foil system, which was designed using an iterative computer procedure based on conventional sub-cavitating 3-D hydrofoil theory (4,7,8,10,14,15,16) can be seen in Fig. 1.

THE ITERATIVE COMPUTER DESIGN TECHNIQUE

The program treats details of the hydrofoil system design in the form of co-ordinates of each end (A and B) of the foil elements. These are referred to the boat reference system (x,y,z). In addition, details of the chord length at ends A and B, section type and properties, angle of incidence as well as overall details of the craft including the number, weights, and positions of the crew, the position of the centre of gravity and centre of effort of the sails, and overall weight are supplied.

The boat reference system which has its origin at the intersection of the design waterline and the aft perpendicular, is arranged with the +ive x-direction forwards, +ive y-direction to starboard and +ive z-direction downwards. A second system, the earth reference system (X,Y,Z) is arranged with its origin at the intersection of the instantaneous waterline and the aft perpendicular with the +ive y-direction to starboard and +ive z-direction vertically downwards. The difference between the systems is due to the height of flight, and trim, yaw and heel angles. Before the hydrofoil element calculations can be started, the co-ordinates in the boat reference must be transformed to the earth reference system and this is done using the transformation matrix as below:

$$\begin{bmatrix} x \\ y \\ z \end{bmatrix} = \begin{bmatrix} \cos\tau \cos\lambda & \sin\lambda \cos\tau & \sin\tau \\ \cos(\pi/2+\lambda) \cos\theta + \cos\lambda \sin\theta \cos(\pi/2+\tau) & \cos\lambda \cos\theta + \sin\lambda \sin\theta \cos(\pi/2+\tau) & \cos\tau \sin\theta \\ \cos(\pi/2+\lambda) \cos(\pi/2+\theta) + \cos\lambda \cos\theta \cos(\pi/2+\tau) & \cos\lambda \cos(\pi/2+\theta) + \sin\lambda \cos\theta \cos(\pi/2+\tau) & \cos\tau \cos\theta \end{bmatrix} \begin{bmatrix} x \\ y \\ z \end{bmatrix} = \begin{bmatrix} 0 \\ 0 \\ z_0 \end{bmatrix}$$

HIGH-SPEED SURFACE CRAFT

where τ = angle of trim +ive bow up
 θ = angle of heel +ive to Port
 λ = angle of yaw +ive to Port
 Z_o = height of flight at the z axis.

For each value of forward velocity and from initial values of τ , θ , λ and Z_o , the program calculates and sums lift, drag and side force.

$$\text{Total Lift} \quad L = \sum_{i=1}^n \ell_i$$

$$\text{Total Drag} \quad D = \sum_{i=1}^n d_i$$

$$\text{Total Side Force} \quad SF = \sum_{i=1}^n sf_i$$

where ℓ_i , d_i , sf_i are the lift, drag and side force on foil element i
 n = total number of foil elements.

A comparison is then made between the total lift and the all up weight and a correction made to Z_o accordingly:

$$< \quad \rightarrow (Z_o)_N = (Z_o)_O - \Delta Z_o$$

$$\sum_{i=1}^n \ell_i = W_b + W_c \quad \rightarrow (Z_o)_n = (Z_o)_o$$

$$> \quad \rightarrow (Z_o)_n = (Z_o)_o + \Delta Z_o$$

where W_b = Boat weight

W_c = Crew weight

subscripts n and o denoting new and old values respectively.

Longitudinal equilibrium is then considered, the trim angle being adjusted until the forces from the various foil units are balanced with the forward thrust from the sails:

Assuming a quasi-steady condition exists where the forward thrust from the sails equals total drag then taking moments

$$\sum_{i=1}^{n_b} \ell_{b_i} < \left(M_o W_c + M_o W_b - M_o \sum_{i=1}^{n_s} \ell_{s_i} - M_o \sum_{i=1}^{n_{st}} \ell_{st_i} + \sum_{i=1}^n d_i \times Z_{cc} \right) / X_{Bow} \quad \rightarrow \tau_N = \tau_o - \Delta\tau$$

$$> \quad \rightarrow \tau_N = \tau_o$$

$$\quad \rightarrow \tau_N = \tau_o + \Delta\tau$$

where ℓ_b , ℓ_s , ℓ_{st} are lifts of bow, side and stern foil elements respectively

n_b , n_s , n_{st} are numbers of bow, side and stern foil elements respectively ($n_b + n_s + n_{st} = n$)

M_o - denotes moment about the origin

Z_{cc} - vertical separation of the centre of effort of the sails and the centre of lateral resistance

X_{Bow} - X co-ordinate of the bow foil unit.

In practice because of the position of the origin,

$$M_o \sum_{i=1}^{n_{st}} \ell_{st_i} = 0$$

When an overall balance is achieved lift, drag and side forces are presented itemised between bow,

HIGH-SPEED SURFACE CRAFT

side and stern foil units, together with lift/drag ratios and the calculated values of height of flight and trim.

With the use of variations of this program, detailed information on coefficients and forces for each foil element can also be obtained.

PERFORMANCE PREDICTIONS

The theoretical curves of drag, trim and vertical displacement at the origin for 'Kaa' and 'Mayfly', at zero heel and yaw angles, are presented in Figs 3,4,5. The 'Mayfly' curves are based on an estimate of her foil configuration and probably underestimate drag. The two boats are not directly comparable, 'Kaa' having a greater displacement and sail area, but a comparison can be obtained in terms of the non-dimensional factor:

$$S = \sqrt{S_A/3\sqrt{V}} \quad \text{or} \quad \left[S = \frac{S_A^{1/2}}{V^{1/3}} \right]$$

where S_A = sail area

V = volumetric displacement.

This for the two boats is very similar. The values are 6.6 for 'Mayfly' and 6.7 for 'Kaa' when sailed single-handed.

It can be seen in Fig. 3 that once the boat takes-off, drag does not increase further until the velocity reaches a value around 10-11 m/s. This is because as the boat accelerates wetted surface area is reduced, but above this speed, drag increases more sharply as the boat flies even higher and the aspect ratio reduces and surface effects become more influential.

It might be presumed from these curves that the boat would immediately accelerate after taking off to a velocity around 10-11 m/s, but this is not the case because of:

- (1) Yaw and Heel effects on drag.
- (2) The sails do not provide constant power.

The speed increase causes the apparent wind angle to the boat's course to be reduced. This means that great care must be taken with the set of the sails to ensure their efficient operation. In these conditions, the sails are operating at lower angles of incidence and the ratio of heeling force/driving force is increased, so although the higher apparent wind speed produces greater forces from the sails, the driving force component does not increase in proportion.

THE WEYMOUTH FOIL SYSTEM

Two main defects in this foil arrangement became apparent at the Weymouth trials:

- (1) Angles of incidence of the bow and side foil units although near to their ideal values were too low to deal with full scale operation in wave motions.
- (2) The side foil unit required redesigning from a structural point of view.

Analysis of the Weymouth foil system showed a high initial drag arising from a high value of trim at take-off. The trim curve shows that values remained high throughout the speed range which confirms the first defect.

Some full scale trial results are shown plotted alongside the theoretical curves in Figs 4,5. These were taken from the photographic and video tape records and show how the actual trim values are even higher than the predicted values by, an average of 1 degree. The height of flight results show the general form of the prediction although there is a scatter of approximately $\pm 0.1m$.

FOIL SYSTEM BB AND BC

The next development involved a new design of the side foil, incorporating only one lifting surface, the element with dihedral angle 40 degrees, set at a greater angle of incidence. This foil is supported by two NACA 16-012 struts of chord length 0.15m. The curves for this configuration are designated BB with two crew and BC with one crew member, and are shown in Figs 3,4,5.

FOIL SYSTEM BD AND BE

There still remained a possibility to reduce the drag hump at take-off. It was found that by remov-

ing the centre foil elements of the bow foil, trim angles would be reduced. This is shown in Fig. 5 by the curves BD and BE again for two and one man crew respectively. Further curves of the lift/drag (L/D) ratio are plotted for the boat with her new foil system with a one man crew and for 'Mayfly' in Figs 6,7. Overall lift/drag for the two boats is very similar. An increase in the side foil (bow foils on 'Mayfly') L/D ratio can be seen as the strut foil intersection clears the water surface.

Inclusion of Heel and Yaw Angles

More realistic predictions are obtained after the inclusion of heel and yaw angles. This is because with any sailing craft, there is a side force component of sail force which requires an equal and opposite side force reaction from the foil system. This combination of forces also results in a heeling moment which must be counteracted. In this case this is achieved by a combination of non-symmetrical foil loading and lateral movement of crew weight.

Curves for various heel and yaw variations for the configuration BE are plotted in Figs 8,9,10,11. These illustrate that:

- (1) Only small angles of heel and yaw are necessary to produce the restoring force, especially at high speeds.
- (2) Heel in isolation would tend to reduce drag.
- (3) Angles of yaw (alone or coupled with heel) increase drag.
- (4) Height of flight and trim are insensitive to heel or yaw until the higher angles of heel are reached (above 5°).
- (5) Angles of heel make a significant contribution to side force generation.
- (6) The side force generated by an angle of yaw is fairly constant over the speed range.

Since heel is unlikely to occur in the absence of yaw, the overall effect is an increase in drag. The reduction in drag due to heel occurs largely because of the corresponding increase in aspect ratio and hence lift/drag ratio of the leeward foils which carry more of the total weight as speed increases.

There is a balance between each angle of yaw, heel, drag and side force, but this is more complex than that between trim and sail thrust force and will depend not only on non-symmetrical foil loading, but also on the crew positions. The ratio of side force/drag is also important in assessing boat performance from sail force predictions and the possible boat heading angles to the true wind velocity vector.

Inflexion in the side force curves comes about as the side foil unit struts emerge from the water surface.

HYDROFOIL BOAT MKIII

A further computation was made for the craft described in reference (1). Here the results can be seen in Figs 12,13,14 of drag, height of flight and trim and the agreement with experimental points is encouraging. The drag curve is seen to be overestimated by approximately 10%, but the drag hump is correctly simulated. If allowance is made for the buoyancy of the immersed hydrofoils, a reduction in the all-up weight supported by hydrofoil lift can be made of approximately 5kg, this on an all-up weight including the crew of 122kg effectively reduces drag in proportion (i.e. by 4%). The Reynolds No. at the hump speed is 4×10^5 which is in the transitional region between sub- and super-critical flow regimes. A slight reduction in the drag coefficient would be expected in this region and this could account for the remaining discrepancy, (see section on The Model).

Bow Foil - Large Heel and Yaw Angles

The force situation on the bow foil was calculated for larger values of heel and yaw at an arbitrary speed of 12 ms^{-1} . It was desired to compute these values with a view to the possible use of the bow foil as a supplementary steering device. While lift is seen to drop with heel and yaw, the reductions are not dramatic, although in a similar range the drag due to yaw is seen to increase considerably. Side force increases linearly with angles of yaw and heel, but is much greater with yaw. See Figs 15,17.

PROPOSED TESTS ON THE 1/4 SCALE MODEL

Tests on a 1/4 scale model of the craft are planned to verify further the theoretical work. These are complicated by the normal procedure associated with testing sailing craft accentuated in this case by the high carriage speeds involved. A study was made of previous sailing yacht tests (11,12,13) in order to ascertain a satisfactory test procedure and it was realised that the model would

HIGH-SPEED SURFACE CRAFT

require to be towed by a specially designed dynamometer. The problems faced involve an inter-relation between the lateral and vertical components of sail force dependent on the angle of heel. Coupled with this is the necessity to tow the model from an assumed centre of effort position (assumed fixed for convenience), an ability to select angles of yaw and to allow freedom to simulate flight conditions.

The Dynamometer

The dynamometer design is shown in Fig.16. Side force, drag (these are actual values at zero yaw angle, but require correction when yaw $\neq 0$) and yaw moment can be measured by strain gauged bars, yaw by means of a scale or electrically using a potentiometer, heel by means of an inclinometer and vertical displacement by linear inductive transducers. The design of the dynamometer allows side force and drag to be measured at the position of the centre of effort of the sails. The model is allowed freedom to heel and trim, but by means of a universal joint between the model's mast and the strain bar of the dynamometer, a restriction in yaw is achieved. Yaw can be set before a run or adjusted as described below, and by this means yaw moment can also be measured. One difficulty is that the measurement of yaw angle is slightly in error because of the deflection of the yaw moment strain bar. This is assumed to be slight. A similar principle is used for the tests in reference (12). Taking the two orthogonal forces on the strain towing bar as X and Y, we have:

$$\text{Drag} = X \cos \lambda + Y \sin \lambda$$

$$\text{Side Force (L)} = Y \cos \lambda - X \sin \lambda$$

where λ = angle of yaw (+ve to starboard).

Also if W is the downwash component of the sail force,

$$W = L \tan \theta$$

where θ = angle of heel.

Hence if W is set constant for a run, we have:

$$W = (Y \cos \lambda - X \sin \lambda) \tan \theta = \text{const.}$$

but, X, Y, and θ all reach steady values for a given angle of yaw (λ) so the problem is to set the correct angle of yaw for the run.

In the initial design it was proposed to operate the dynamometer completely by automatic means. This was to be achieved by setting the downwash sail component previous to the run and electrically measuring side force, drag, heel and yaw angles and then to compute a yaw angle correction which was to be adjusted by means of a servo motor rotating the dynamometer. For the first tests, however, a manual operation will be used and an interpolation carried out for the correct yaw angle. Such considerations are only necessary, of course, when heel is non-zero.

Manually

To make a run manually the downwash component of sail force is off-loaded from the scale pan and an angle of yaw set. During the run after steady state conditions have been reached readings are taken of side force, drag, heel angle and height of flight. Similar runs are repeated at different yaw angles and the correct results obtained by interpolation. At low speeds adjustments to the yaw angle might be made manually during a run, but because of the length of the tank this is not envisaged at higher speeds.

Electrically

By this means, it is merely necessary to unload the downwash sail component and set the yaw angle near to that anticipated during the run. The new yaw angle will be computed and set automatically although at higher speeds the few seconds at steady run conditions may not allow a steady yaw angle to be reached.

The Model

Table II gives relations between the model and full scale craft. The model foils are not exactly similar to the full scale craft in order to facilitate manufacture, their sections being mainly circular arc, ogives and biogives. If both the model and the full sized vessel are operating in the same water, the kinematic viscosity (ν) is constant and the full scale Reynolds No. is 8 times the model value. Actual values of this parameter are given in Table II from which it can be seen that while the model foils are operating in the sub-critical flow region, the full scale hydrofoils are

still in the transitional regime and this comes about because of the relatively low speed operation of, and small chord lengths used, in sailing hydrofoil craft. Turbulence stimulation is normally effective from the transitional to the super-critical regions, where an increase in the drag coefficient is experienced, the effect in the sub-critical region of the stimulators merely being to increase the parasitic drag (8).

An allowance for Reynolds No. is made in the friction coefficient based on the ITTC line but this does not model the transitional zone, where drag coefficients would be less. Drag predictions from the model tests can therefore be expected to be slightly pessimistic compared to full scale operation. See Fig. 18, drag curve and ITTC line.

CONCLUSION

A design for the foil system of a sailing hydrofoil trimaran has been developed. Theoretical predictions for this system have been obtained using a development of conventional sub-cavitating hydrofoil theory to a hydrofoil element of constant dihedral angle and varying chord. An iterative computer design technique orientates the boat relative to the earth co-ordinate system taking into account, height of flight, trim, heel and yaw. Forces from the elements of the foil system are then summed for each value of velocity. It was found that:

- (1) Theoretical predictions for a previous sailing hydrofoil boat were compared with experimental tank tests. In general, the agreement was good.
- (2) The developed foil system design compares favourably in terms of drag, height of flight, trim and L/D ratio with the successful craft 'Mayfly'.
- (3) The four point suspension provided by the four foil units is seen to be a stable system.
- (4) Small angles of heel and yaw do not significantly affect drag, height of flight or trim. These same small angles produce large side and heel restoring forces.
- (5) There was reasonable agreement between predicted values of height of flight and trim and the open water trials results over the speed range recorded.
- (6) A study of the effect of large angles of heel and yaw on the bow foil showed that while lift was reduced slightly, the drag doubled for an increase in yaw of 10 degrees.

A more complete experimental program is planned on a 1/4 scale model. If adequate financial support can be found, further full scale trials will be undertaken also.

ACKNOWLEDGEMENTS

The authors would like to thank all those who have helped with the project, including the staff and technicians of the Glasgow University Hydrodynamics Laboratory.

The donation of materials for the original construction of the full scale craft from Scott Bader & Co. Ltd., Fibreglass Ltd. and Unitex Marine, was also very much appreciated.

REFERENCES

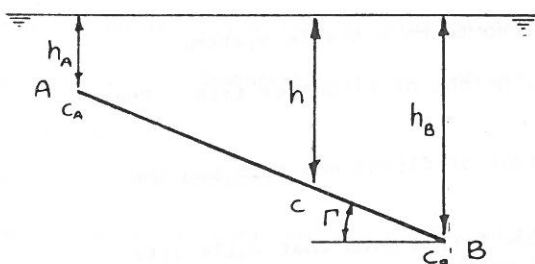
1. Bose, N., 1978 "Design and Development of a Sailing Hydrofoil Vessel", Glasgow University Report NAOE-FYP-78-01.
2. McGregor, R.C., 1980 "Recent Hydrofoil Studies at the University of Glasgow", High Speed Surface Craft, January 1980.
3. Bose, N., 1979 "Initial Sailing Trials of a Hydrofoil-Supported, Wind-Propelled, Trimaran", Glasgow University Report NAOE-HL-80-03.
4. Eames, M.C., 1974 "High Speed Small Craft", Du Cane, P., (Editor), David & Charles, Newton Abbot, Devon.
5. Conolly, A.C., 1966 "Designing for Cavitation Free Operation on Hydrofoils with NACA 16-Series Sections", J. Aircraft, 1966, Vol. 3, No. 6.
6. Eames, M.C., Jones, E.A., 1971 "H.M.C.S. Bras D'Or - An Open Ocean Hydrofoil Ship", Transactions RINA, Vol. 113.
7. Glauert, H., 1948 "The Elements of Aerofoil and Airscrew Theory", Cambridge.
8. Hoerner, S.F., 1958 "Fluid Dynamic Drag", Hoerner Fluid Dynamics, Brick Town, N.J.

9. Riegels, Dr. F.W., 1961 "Aerofoil Sections", Butterworths.
10. Chapman, R.B., 1972 "Spray Drag of Surface Piercing Struts", AIAA Paper No. 72-604, July 1972.
11. Davidson, K.S.M., 1936 "Some Experimental Studies of the Sailing Yacht", Transactions SNAME, Vol. 44.
12. Aflan, J.F., Doust, D.J., Ware, B.E., 1957 "Yacht Testing", Transactions RINA, 1957, 136.
13. Crago, W.A., 1963 "The Prediction of Yacht Performance from Tank Tests", Transactions RINA, Vol. 105.
14. Eames, M.C., Jones, E.A., 1979, Private Correspondence.
15. Hoerner, S.F., Borst, H.V., 1975 "Fluid Dynamic Lift", Hoerner Fluid Dynamics.
16. Breslin, Dr. J.P., 1957 "Application of Ship Wave Theory to the Hydrofoil of Finite Span", Journal of Ship Research, Vol. 1, No. 1, April 1957.

APPENDIX

Hydrofoil Element Theory

The basis of the force calculations for lift, drag and side force are made in the most general case on a hydrofoil element of constant dihedral angle, but varying chord length.



$$\text{Chord length } c = C_A - \frac{(C_A - C_B)(h - h_A)}{(h_B - h_A)} \quad \dots (1)$$

where $h_B > h_A$

C_A & C_B - chord lengths at ends A and B.

Lift forces were calculated taking the ideal 2-D lift curve slope $\frac{C_L}{\alpha_i} = 2\pi$, α_i - angle of incidence, and accounting for the various factors which reduced this below its ideal value (4). Since lift is defined in the vertical plane, the angle of incidence must first be corrected for dihedral angle and then angle of sweep.

$$\alpha_i = \alpha_T \cos \Gamma \cos \gamma$$

where α_T - angle of incidence in the vertical plane

Γ - angle of dihedral

γ - angle of sweep.

Considering the inverse of the lift curve slope, corrections are made as follows:

$$\frac{\alpha_T}{C_L} = \frac{1}{2\pi \cos \Gamma \cos \gamma} \left(\frac{1}{\bar{K}} + \frac{2}{A^2} \right) + \bar{W} + \frac{1 + \bar{\sigma}}{\pi A}$$

and to the drag equation similarly:

$$C_D = C_{D_0} + C_L^2 \left(\bar{W} + \frac{1 + \bar{\sigma}}{\pi A} \right)$$

where C_L - lift coefficient

C_D - drag coefficient

\bar{K} - correction due to loss of lift near the free surface - mean value over hydrofoil element.

$$\bar{K} = \frac{1}{h_B - h_A} \int_{h_A}^{h_B} \frac{(4h/c)^2 + 1}{(4h/c)^2 + 2} dh$$

\bar{W} - correction due to the formation of waves, again a mean value.

$$\bar{W} = \frac{1}{h_B - h_A} \int_{h_A}^{h_B} \frac{1}{2F^2} \exp\left(-\frac{2h}{cF^2}\right) dh$$

F - Froude chord no $F = v/\sqrt{gc}$

$\bar{\sigma}$ - Finite span correction where σ are Prandtl's finite span biplane factor approximated by Eames to

$$\sigma = \frac{A}{A + 12h/c}$$

Again a mean value is used:

$$\bar{\sigma} = \frac{1}{h_B - h_A} \int_{h_A}^{h_B} \frac{A}{A + 12h/c} dh$$

C_{D_o} - section drag coefficient approximated by:

$$C_{D_o} = 2C_f (1 + 1.2t/c) + 0.011 (C_L - C_{L_i})^2$$

C_{L_o} - ideal lift coefficient

C_f - friction coefficient approximated by the ITTC line

$$C_f = \frac{0.075}{(\log_{10} R_n - 2)^2} \quad R_n - \text{Reynolds No.}$$

t/c - thickness chord ratio

A - Aspect Ratio

The treatment of the aspect ratio of the element was developed from (4,15) which suggested

$$A = \frac{b}{c} \left[1 + \frac{h}{b} \left(\frac{a}{b} \right)^3 \right]$$

for the box plane shown in Fig. 19a.

For the dihedral elements this gives expressions

$$A = \frac{b}{2c} (1 + h/b) \quad - \text{ Figs 19b, 19c}$$

$$A = b/c (1 + h/b) \quad - \text{ Fig. 19d}$$

where h is the depth of the centroid of area and where the restriction $h < b$ applies. For $h \geq b$ the ratio h/b is taken as unity.

A further reduction in aspect ratio is made on foils that cut the free surface, the foils being assumed to have no effect for a depth of 0.1 chord (15).

$$\text{Hence } \Delta A = \frac{-0.1}{\tan \Gamma}$$

Spray drag was treated as a simple addition to the drag of the foil element (8,10).

$$\text{Drag due to Spray} = 0.12 \rho v^2 t^2$$

ρ - density of water

v - Velocity

t - thickness of the foil section.

Finally, since α_T is defined in the vertical plane, care must be taken when considering angle of incidence, trim and yaw changes.

$$\alpha_T = \frac{(\alpha_i + \alpha_o \pm \lambda \sin \Gamma)}{\cos \Gamma} + \tau$$

HIGH-SPEED SURFACE CRAFT

α_0 - zero lift angle

τ - trim angle

λ - yaw angle

The +ive or -ive sign depending on the sign convention.

Calculations for struts and fully submerged horizontal foils were treated in a similar manner.

TABLE I

General Dimensions

L.O.A.	5.00m
LWL	4.46m
Draught - foils extended	1.00m
Beam - to outside of floats	4.00m
Beam - overall including foils	5.36m
Beam - centre-line of floats	3.70m

Sail Areas:

Main (fully battened)	13.94m ²
Jib	5.10m ²
Total	19.04m ² (205 sq.ft.)

Main sail AR = L^2/S_A	5.00
Job AR	5.88

Approx. Displacement - ex crew 220kg

'S' Factor = $\frac{\sqrt{S_A}}{\sqrt[3]{V}}$ 6.7 approx. with one crew

AR - aspect ratio

S_A - sail area

L - sail Luff height

V - volumetric Displacement

TABLE II

	'Kaa' Full Size	1/4 Scale Model
LOA	5m	1.25m
Displacement	342kg	5.4kg
Max. Carriage Speed 6.4 ms ⁻¹	12.8 ms ⁻¹ 25 knots	6.4 ms ⁻¹ 12.5 knots
Max. Foil Chord	0.2m	0.05m
Max. Reynolds No.	2.24×10^6	0.28×10^6
Speed at Take-off	3.6 ms ⁻¹	1.8 ms ⁻¹
Min. Foil Chord	0.1m	0.025m
Min. Reynolds No. (at take-off)	0.32×10^6	0.04×10^6

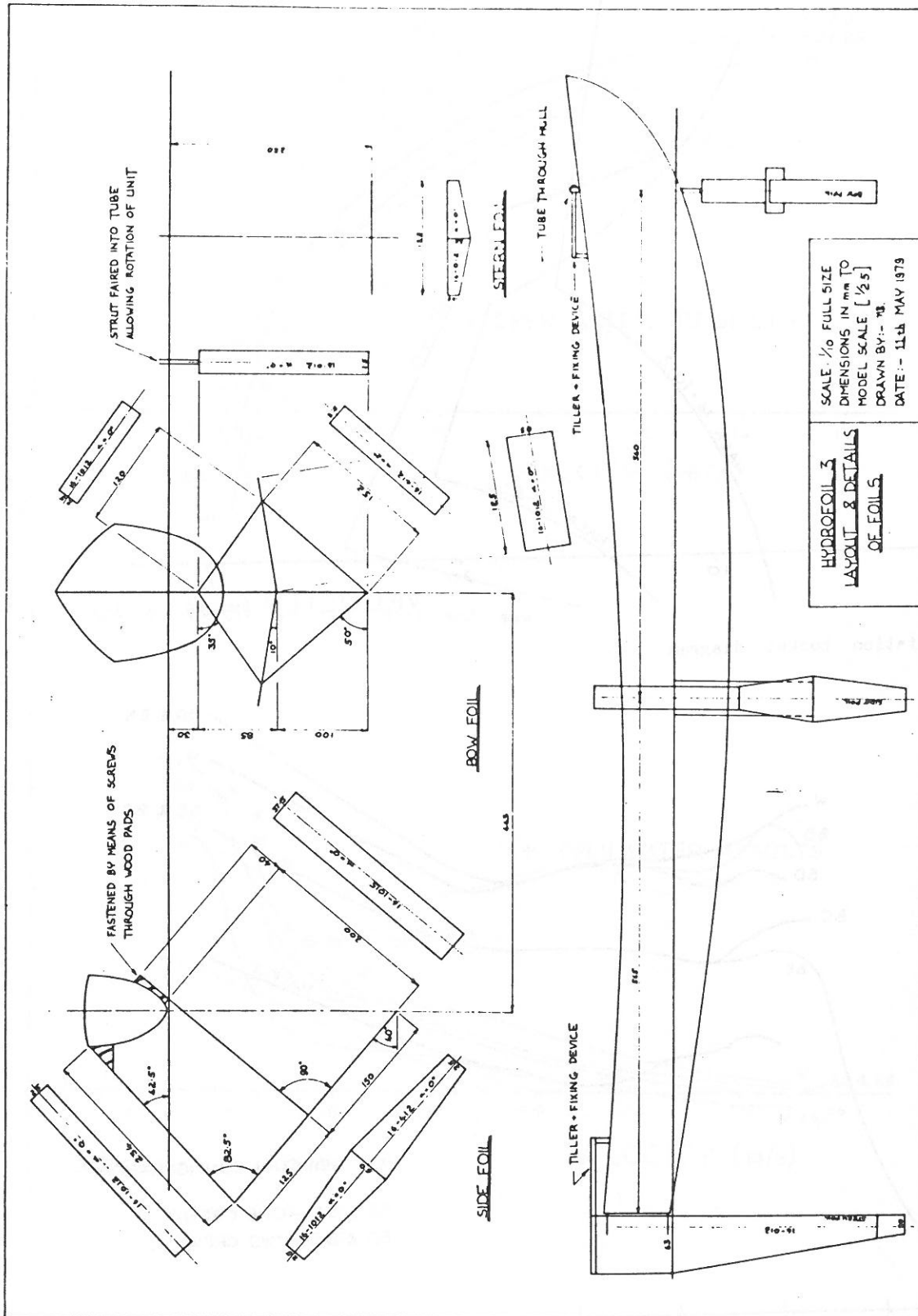


Figure 1 Foil system

HIGH-SPEED SURFACE CRAFT

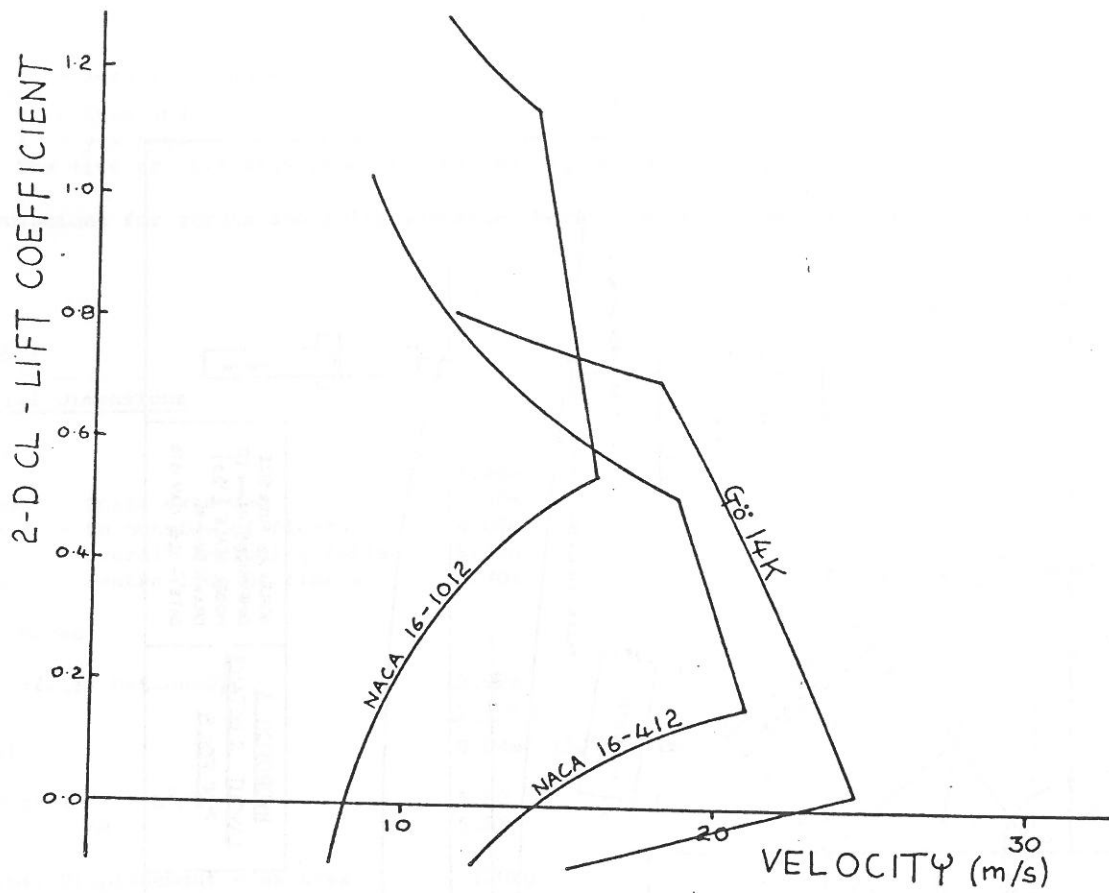


Figure 2 Cavitation bucket diagram

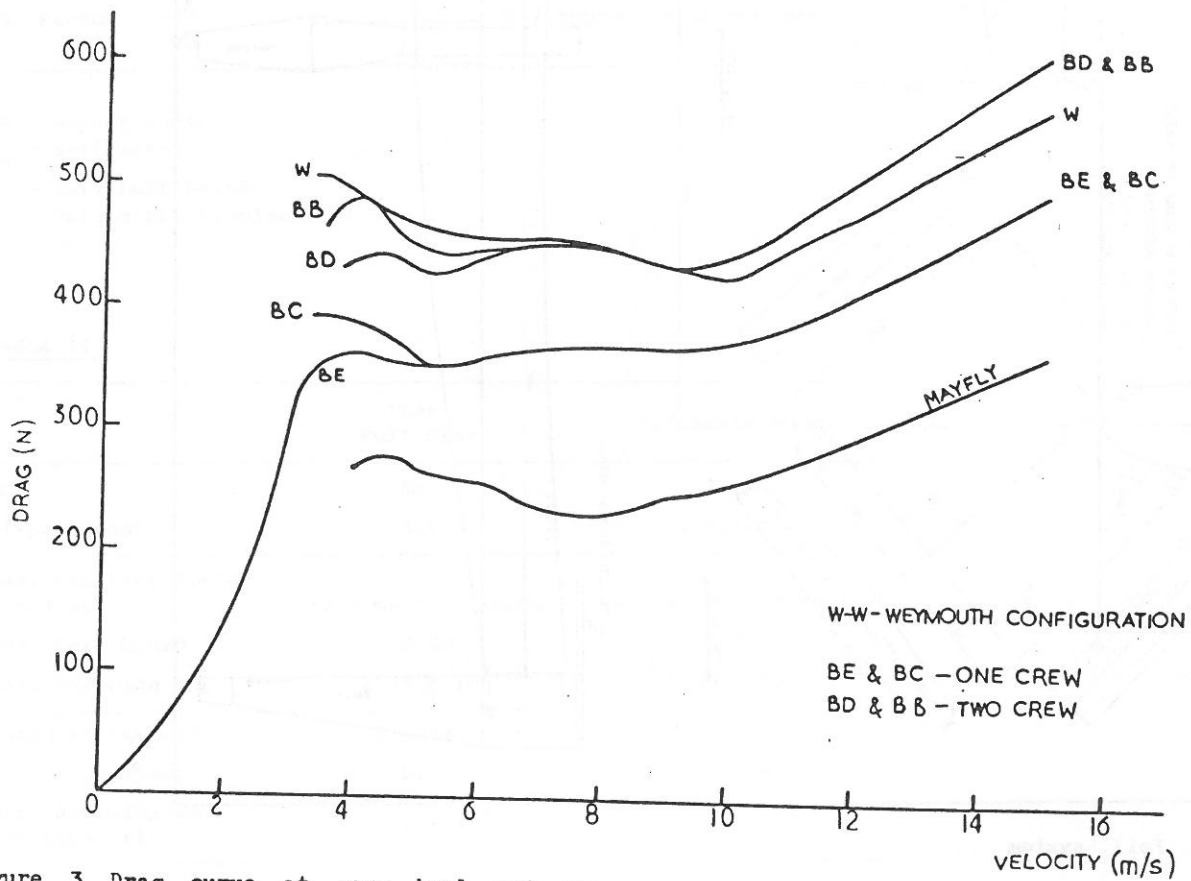


Figure 3 Drag curve at zero heel and yaw

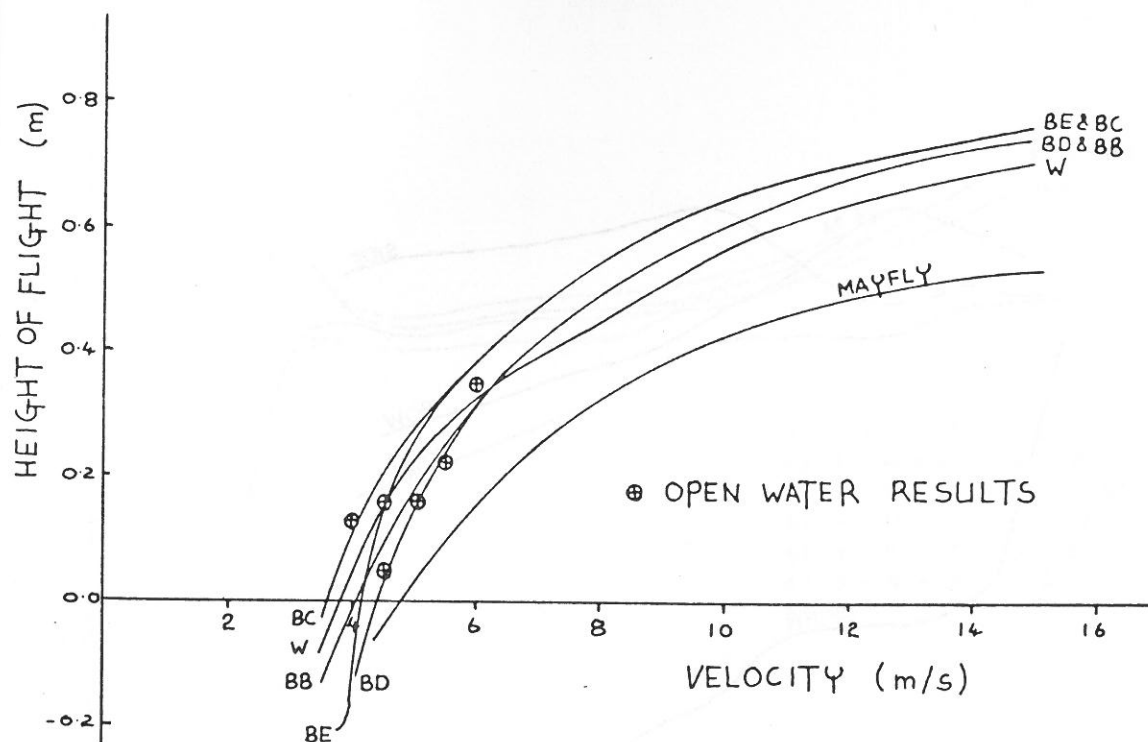


Figure 4 Height of flight at zero heel and yaw

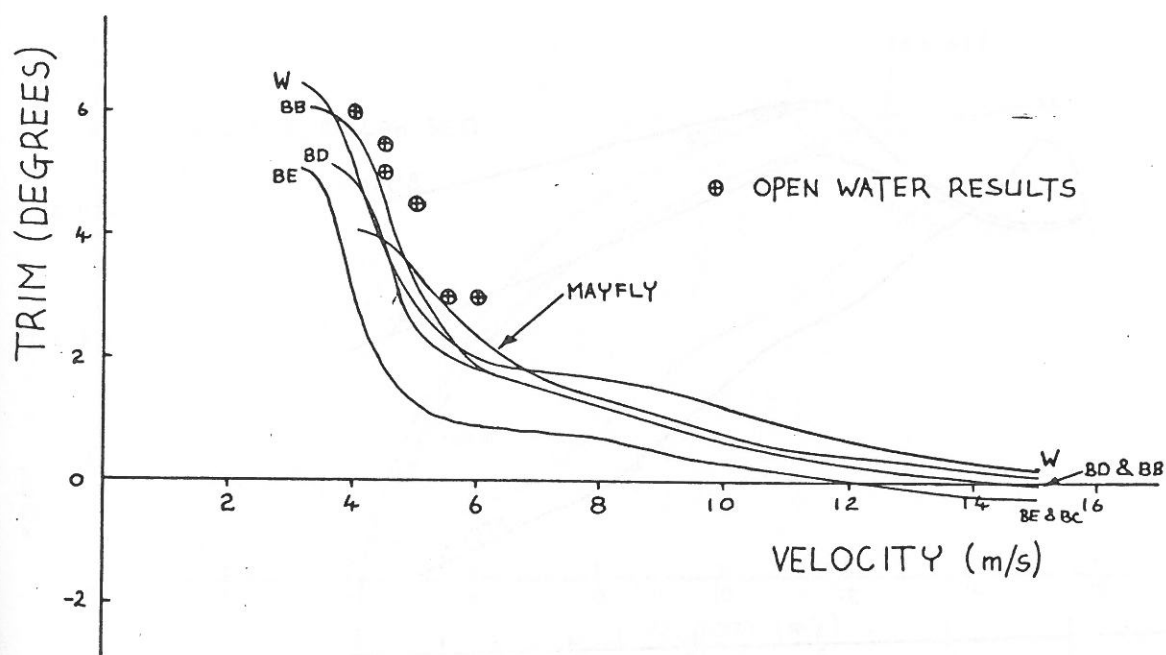


Figure 5 Trim at zero heel and yaw

TRANS 321 19 HIGH-SPEED SURFACE CRAFT

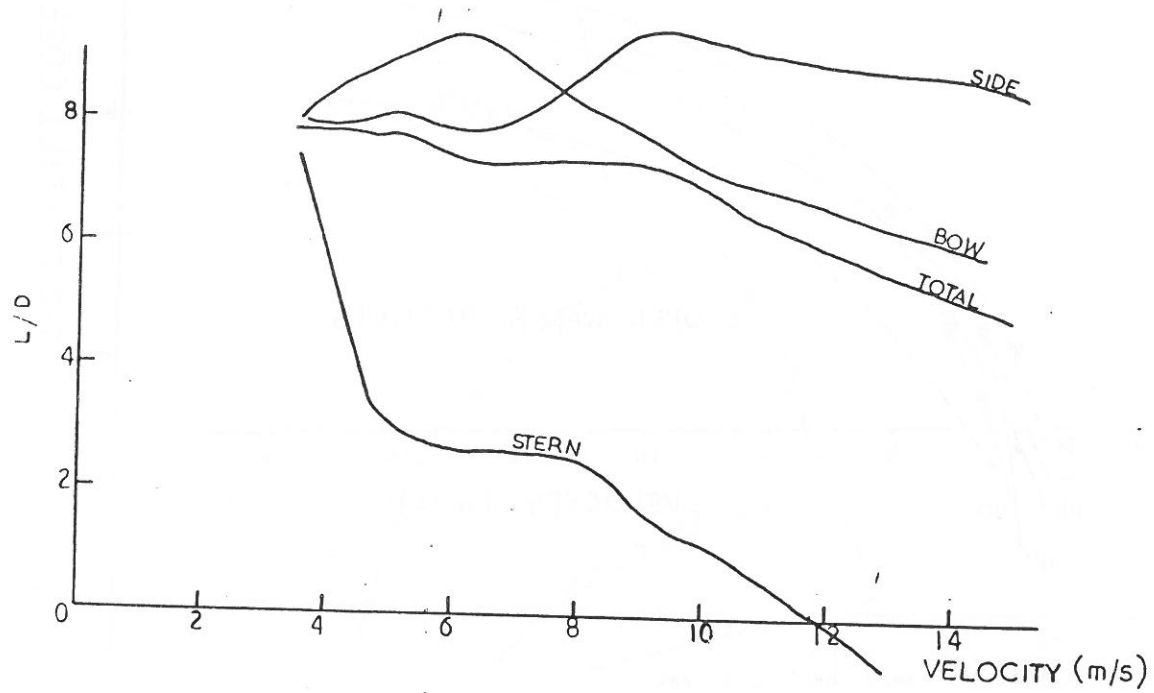


Figure 6 Foil configuration BE - Lift/Drag

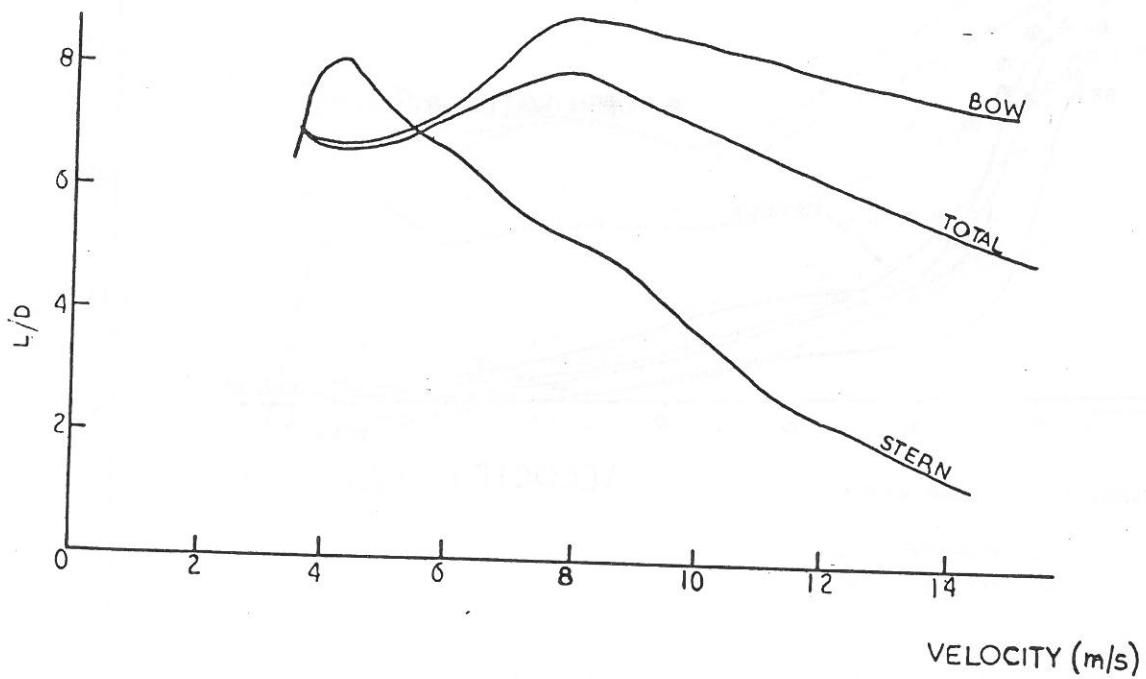


Figure 7 'Mayfly' - Lift/Drag

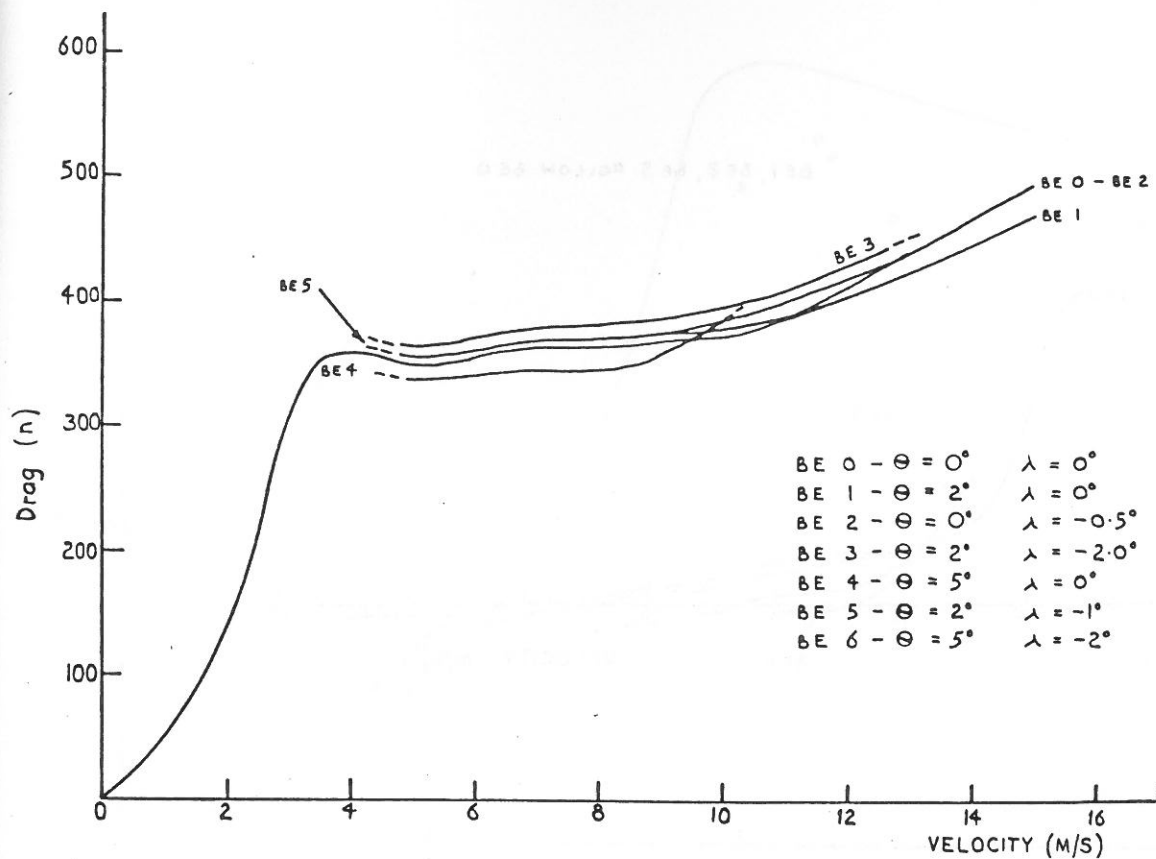


Figure 8 Drag curve - including heel and yaw

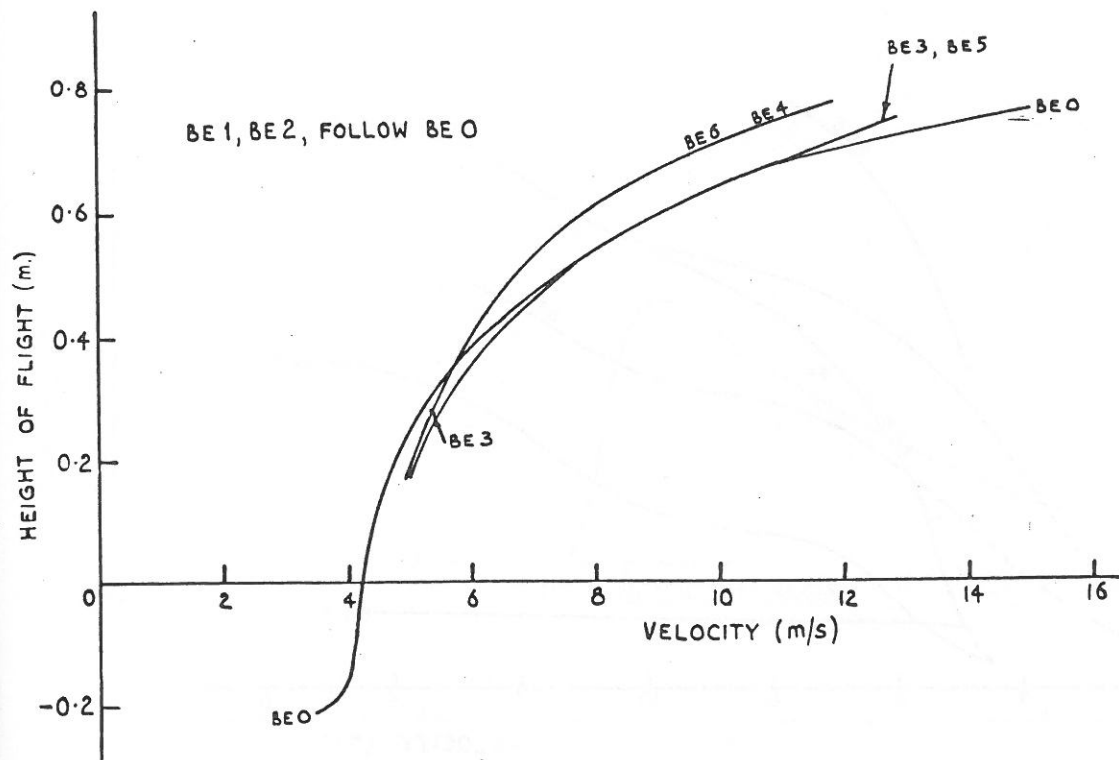


Figure 9 Height of flight - including heel and yaw

HIGH-SPEED SURFACE CRAFT

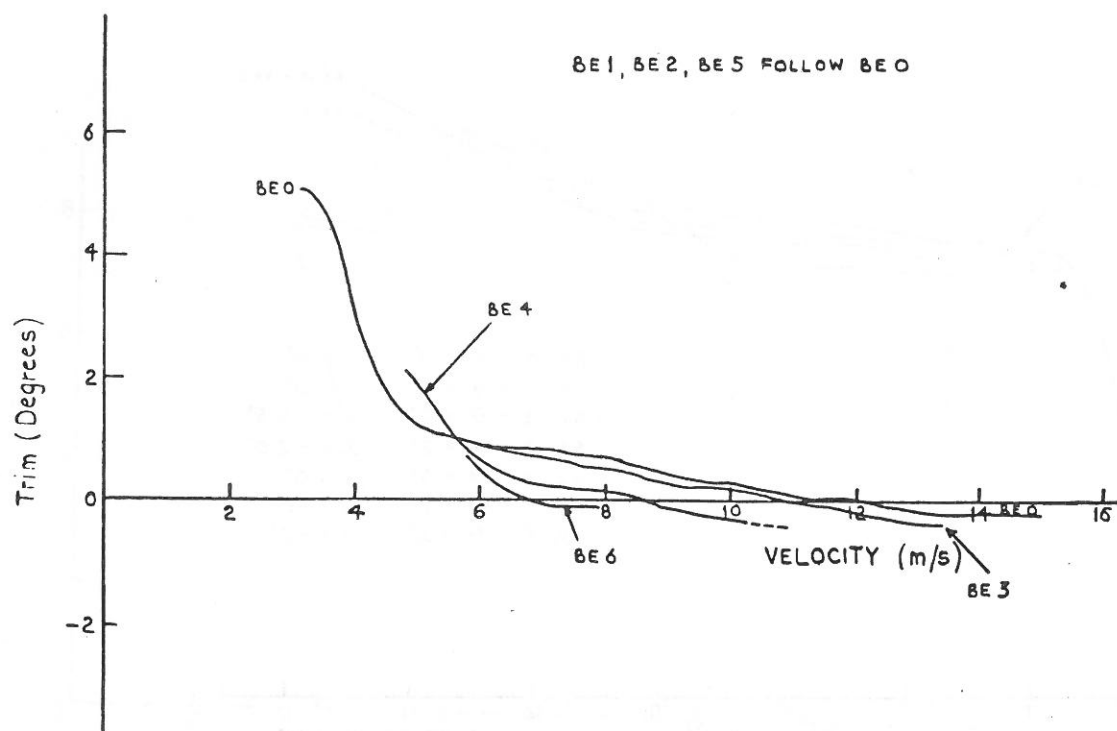


Figure 10 Trim - including heel and yaw

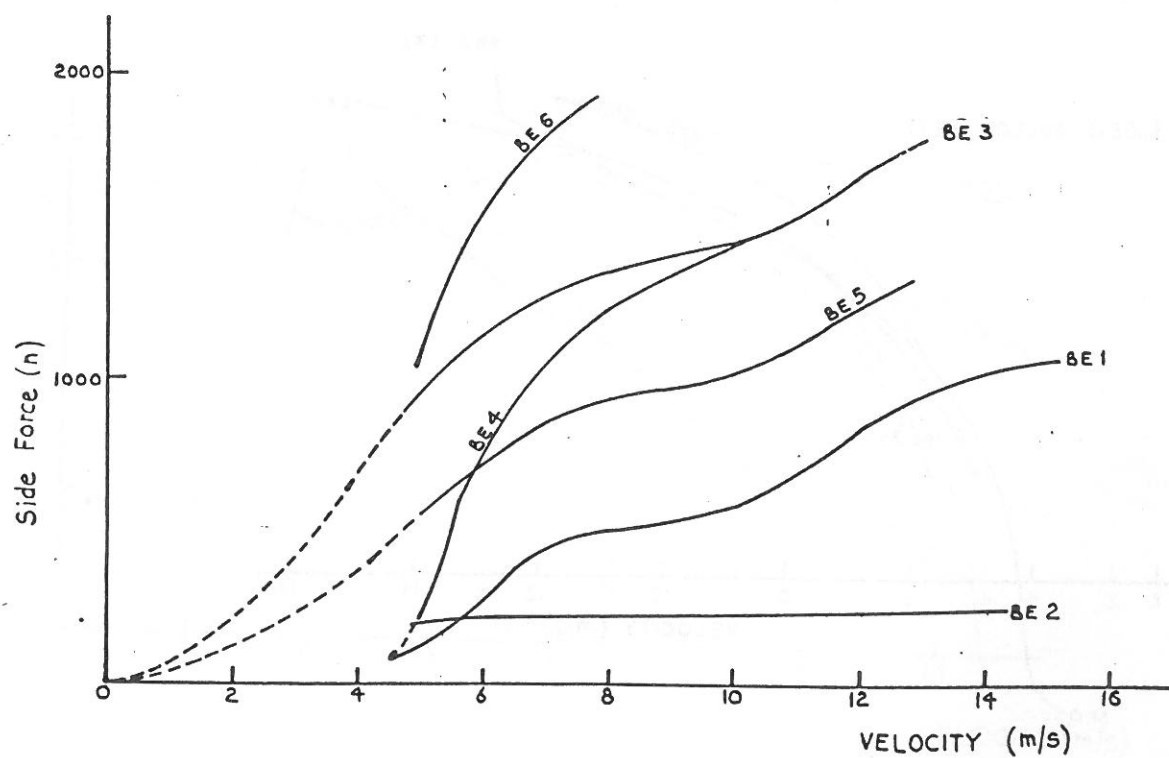


Figure 11 Side Force

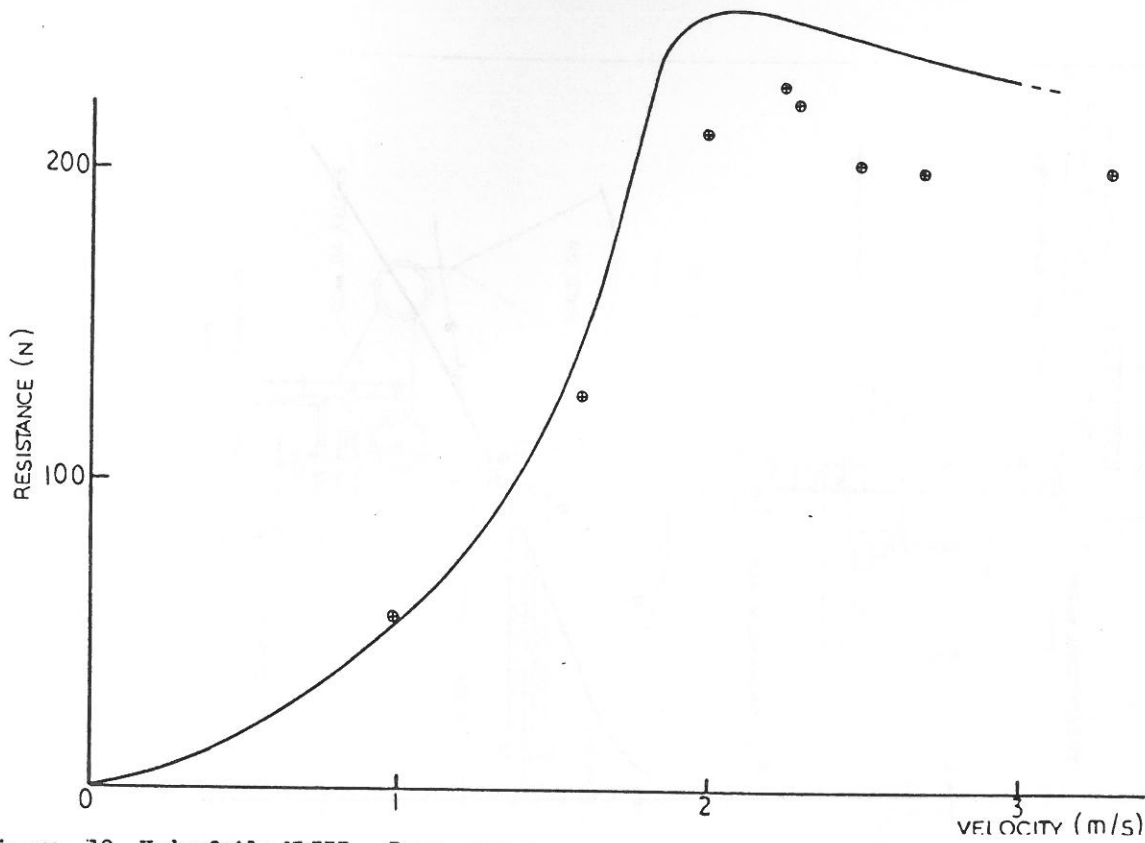


Figure 12 Hydrofoil MkIII - Drag curve

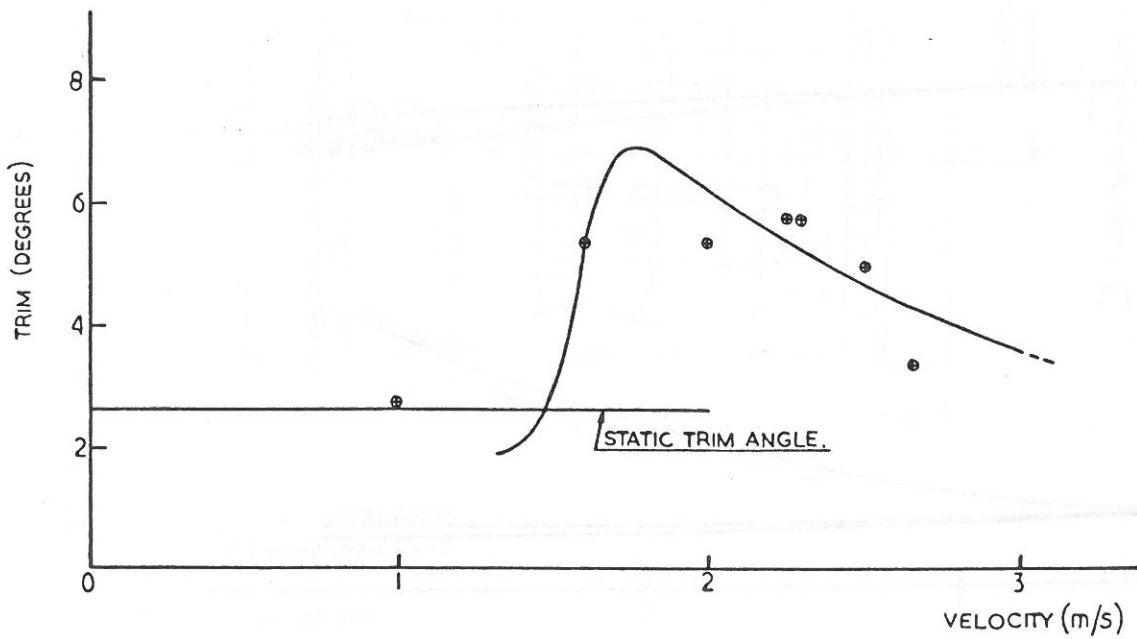


Figure 13 Hydrofoil MkIII - Trim

HIGH-SPEED SURFACE CRAFT

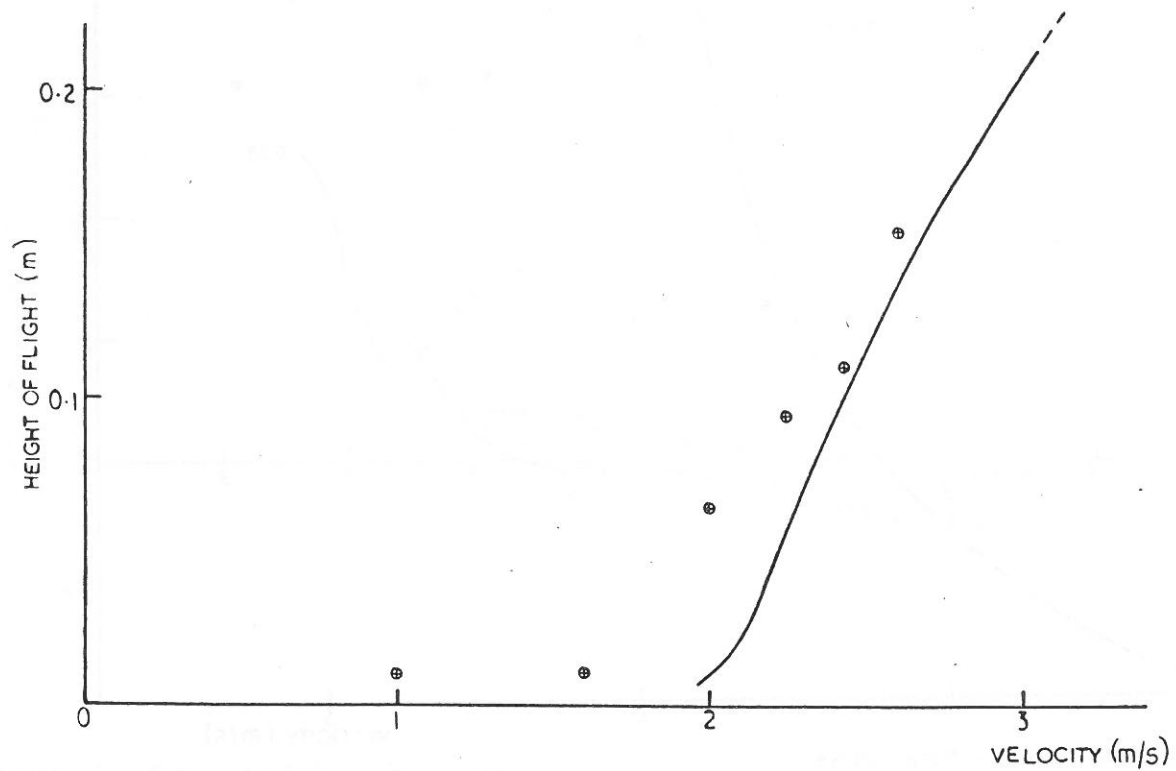


Figure 14 Hydrofoil MkIII - Height of flight

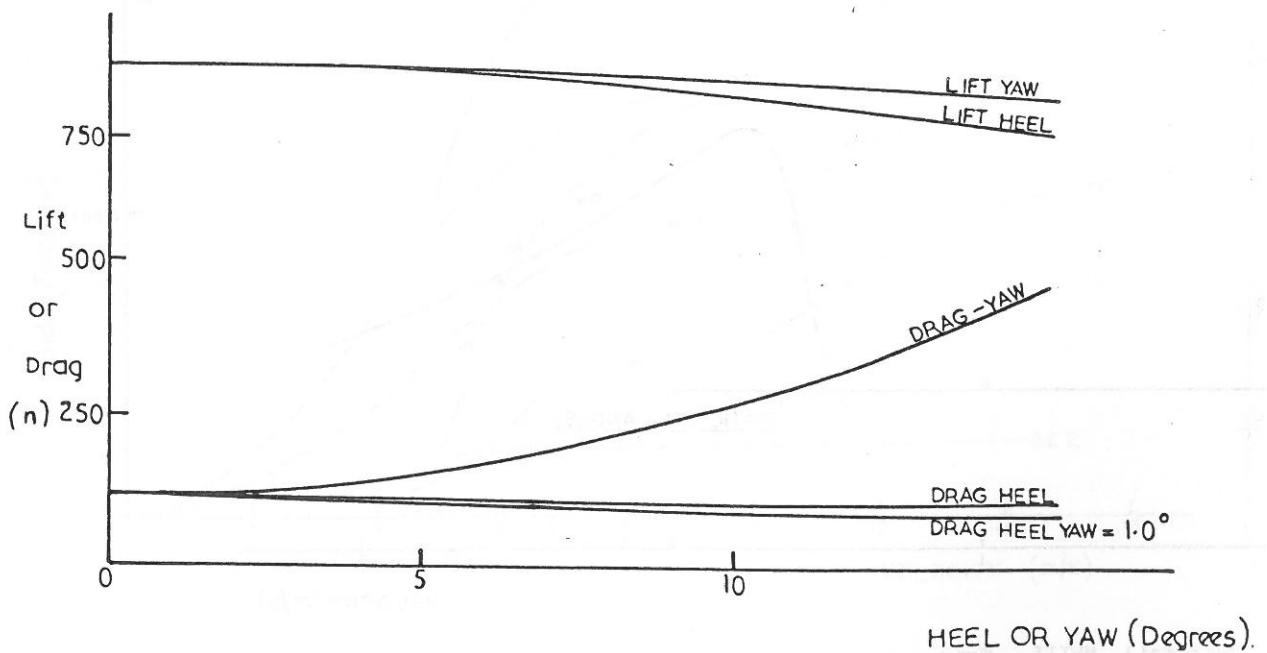


Figure 15 Bow Foil - Lift and drag versus heel and yaw

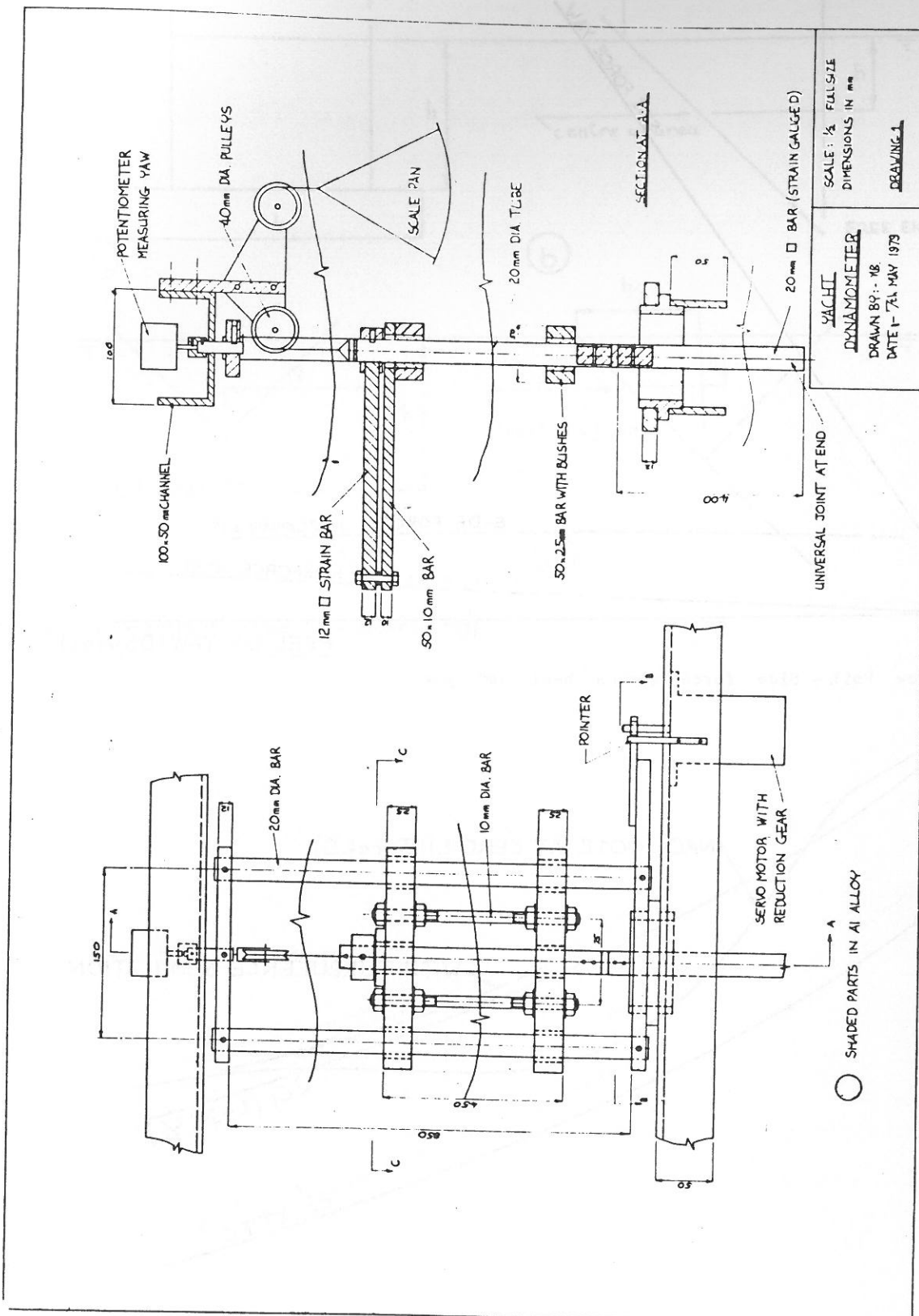


Figure 16 Dynamometer

HIGH-SPEED SURFACE CRAFT

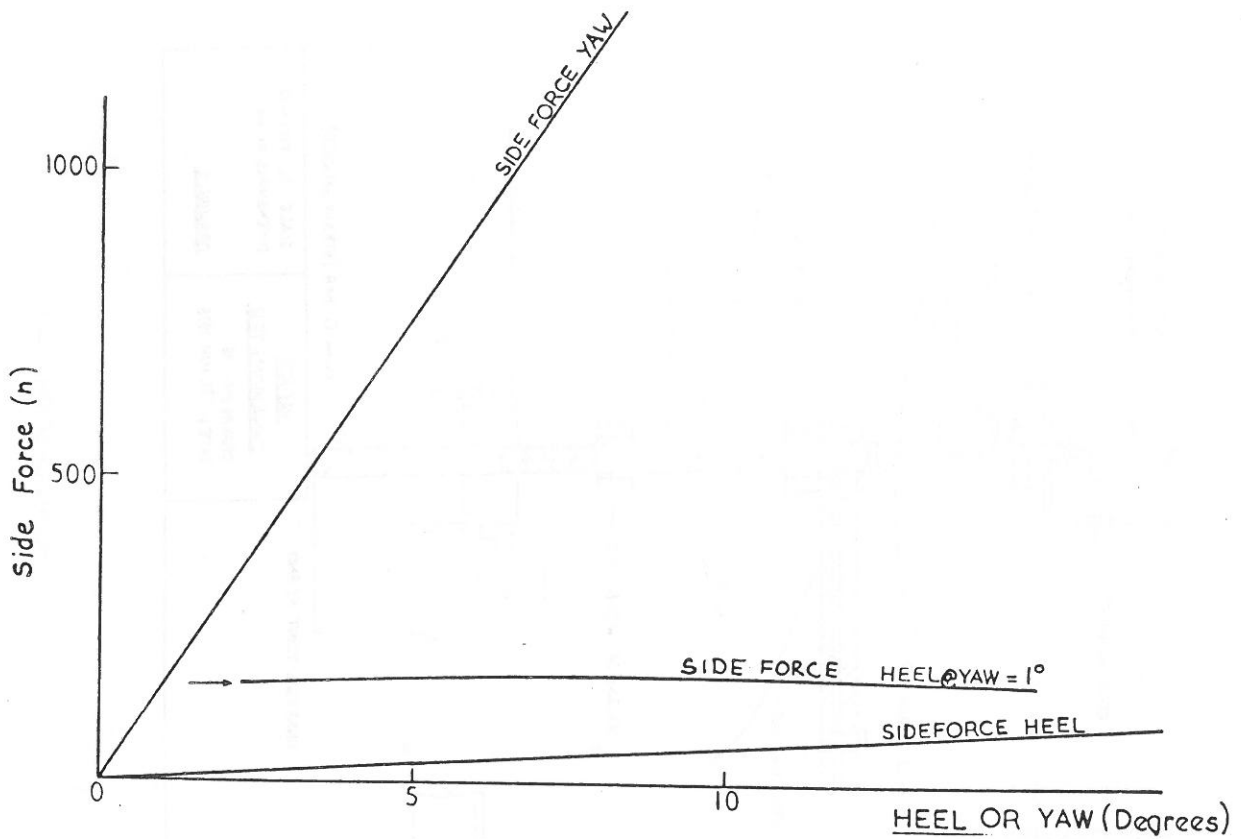


Figure 17 Row Foil - Side force versus heel and yaw

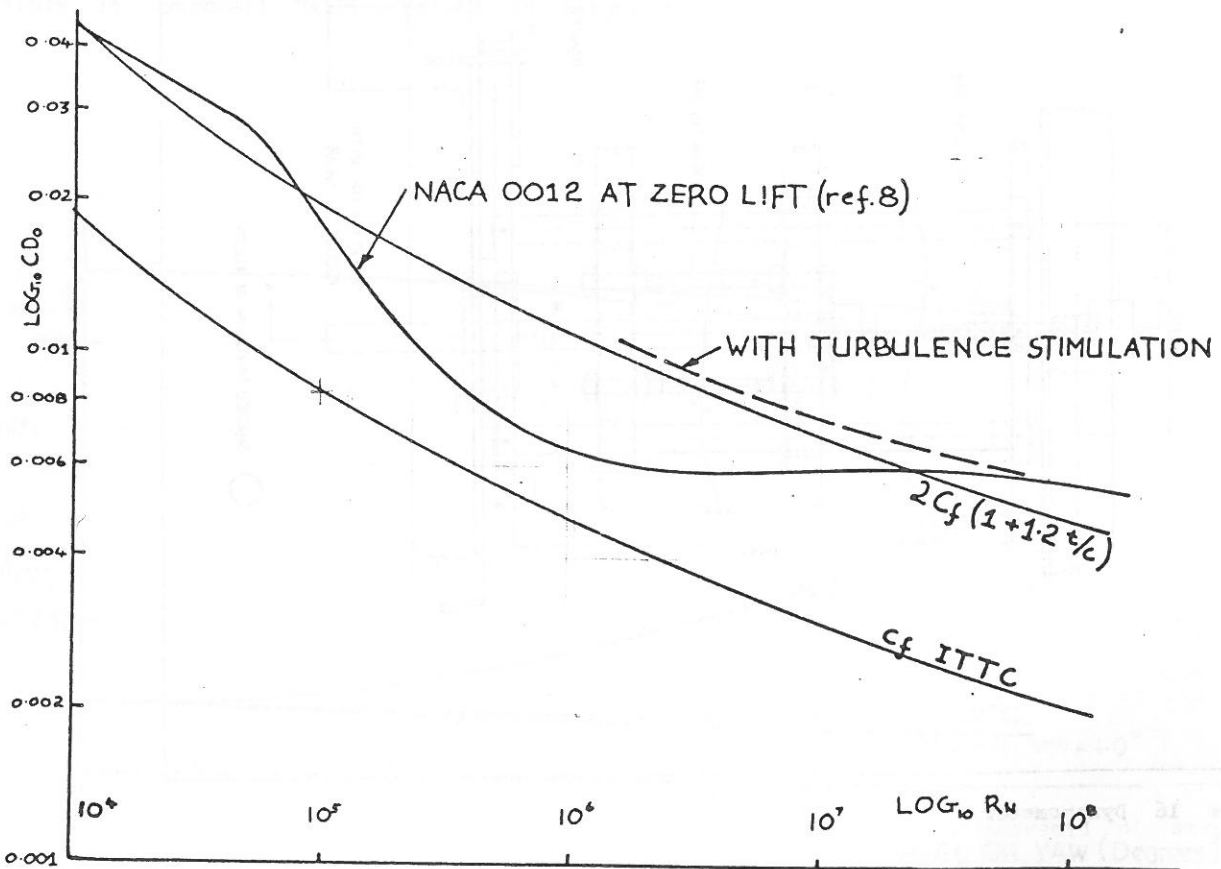


Figure 18 Variation of section drag coefficient with Reynolds No.

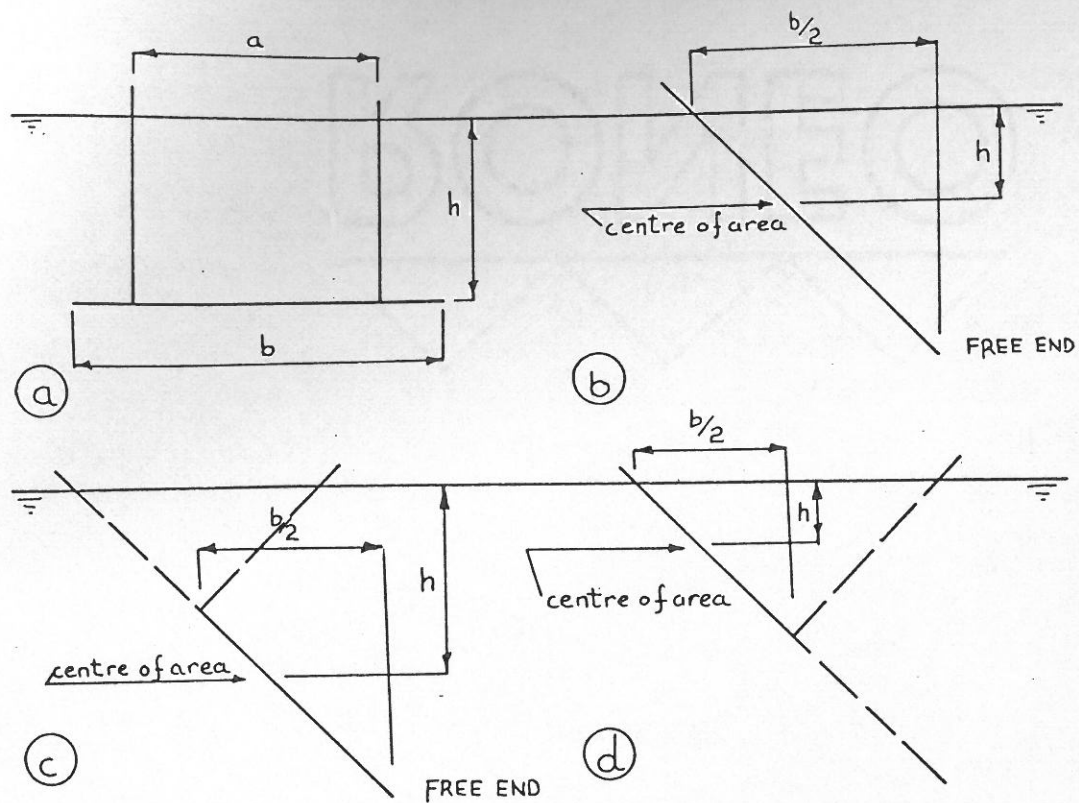


Figure 19 Hydrofoil elements - aspect ratio